Supplementary Figure 1

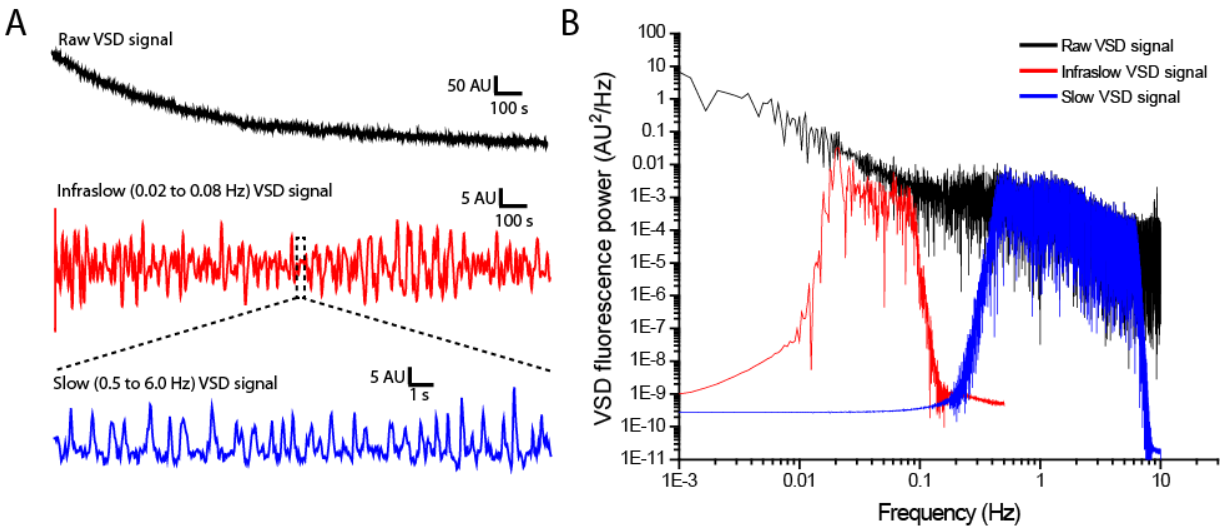

Supplementary Figure 1. Digital filtering of infraslow and slow spontaneous VSD activity.

(A) Top, representative time course of raw VSD fluorescence signal (black) obtained from spontaneous resting state activity derived from an ROI (0.112 mm^2) in primary forelimb somatosensory cortex of an urethane-anesthetized mouse. Middle, infraslow (0.02-0.08 Hz) passband filtered (red) signal in (A, top) illustrating fluctuations in spontaneous activity. Bottom, expansion of segment of VSD signal denoted by dashed line from (A, middle) that has been passband filtered to illustrate fluctuations in slow frequency (0.5-6.0 Hz) spontaneous activity (blue). (B) Power spectra of VSD signals in (A) plotted on log-log axes illustrating highly resolved and distinct separation of infraslow and slow frequency band spontaneous activity.

Supplementary Figure 2

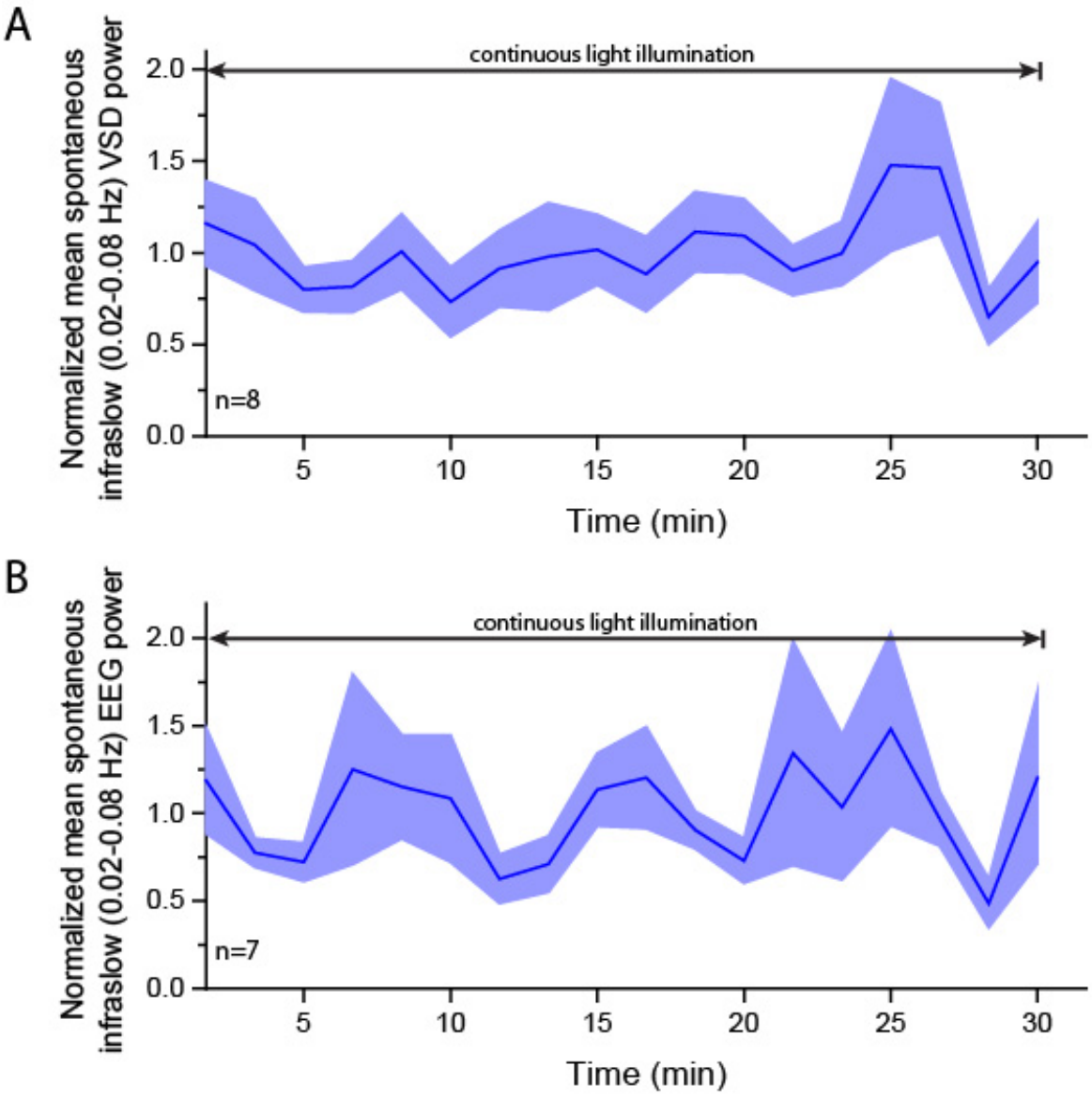

Supplementary Figure 2. Spontaneous infraslow cortical activity is stable during VSD imaging acquisition.

(A) Time course of normalized mean power of spontaneous infraslow VSD activity derived from an ROI (0.112 mm^2) centered on forelimb primary somatosensory cortex (FLS1) during

continuous illumination of VSD. (B) Time course of normalized mean power of spontaneous infraslow EEG activity during continuous illumination of VSD. Shaded regions are S.E.M.

Supplementary Figure 3

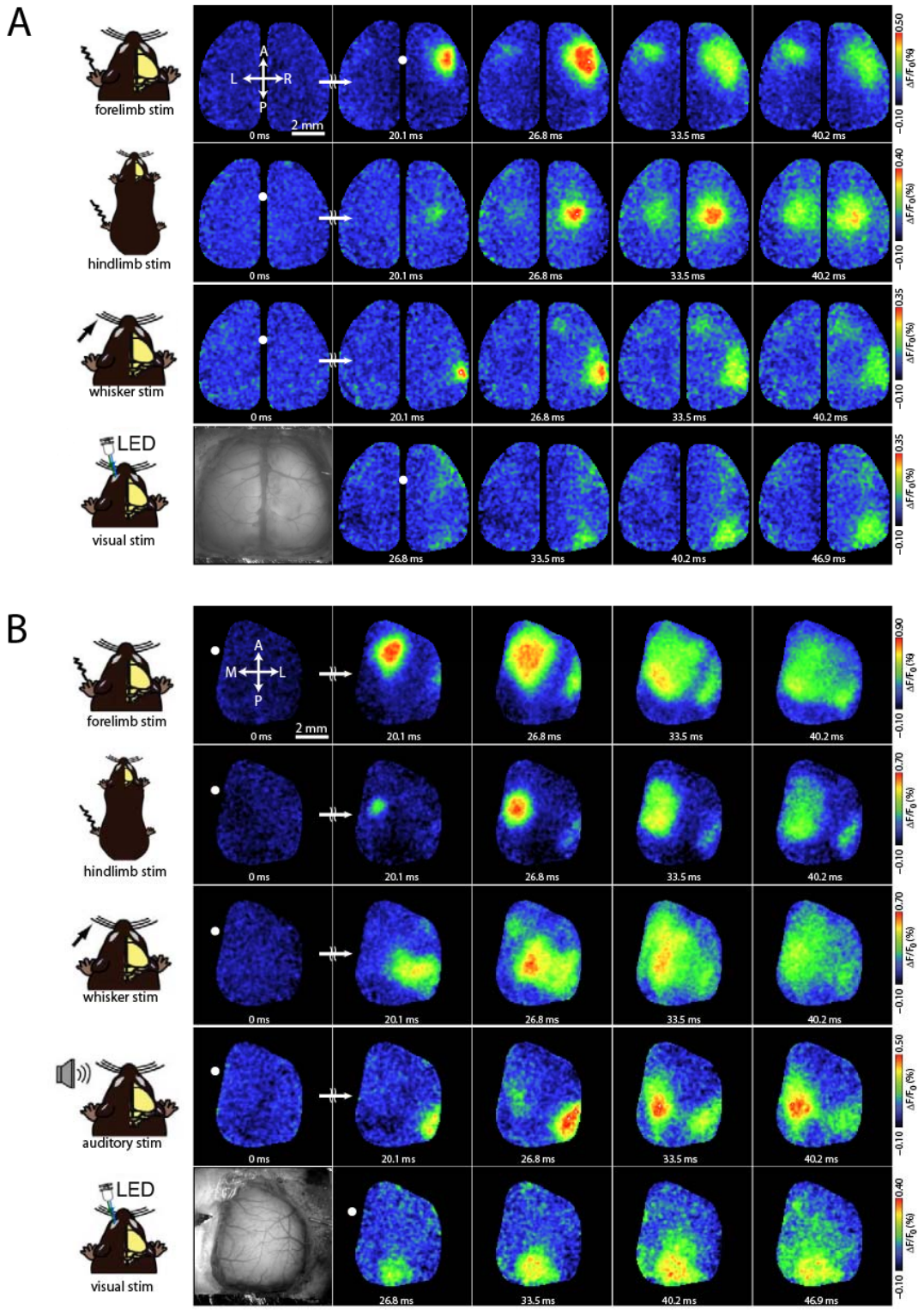

Supplementary Figure 3. VSD functional mapping of the cortex by sensory stimulation.

Functional mapping using the bilateral (A) or unilateral (B) cranial window preparation with multiple modalities of sensory stimulation including forelimb electrical stimulation, hindlimb electrical stimulation, whisker stimulation, auditory tone stimulation, and visual stimulation, as indicated. Montages of evoked VSD activity represent the average of 10 trials of stimulation and are scaled to the adjacent colour bar.

Supplementary Figure 4

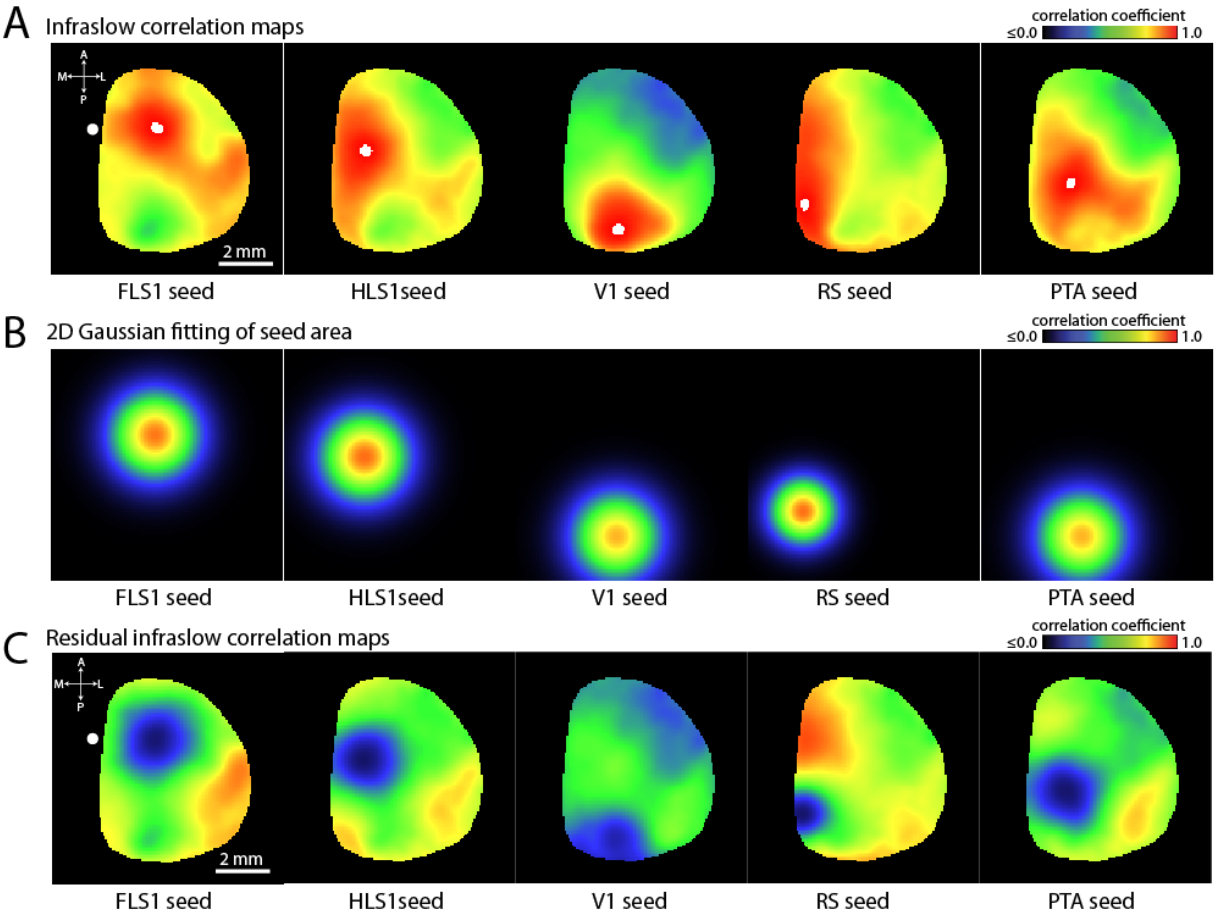

Supplementary Figure 4. Modeling and removal of the contribution of correlation surrounding the seed pixel region.

(A) Correlation maps for seed areas located in forelimb primary somatosensory cortex (FLS1), hindlimb primary somatosensory cortex (HLS1), primary visual cortex (V1), retrosplenial cortex (RS), and parietal association cortex (PTA) and generated from 30 minutes of spontaneous infraslow activity. (B) For the correlation maps in (A), the area of correlation localized around

the seed region was fit with a 2-dimensional Gaussian function. (C) Residual correlation maps resulting from the subtraction of the fitted seed area correlation in (B) from the correlation maps in (A).

Supplementary Figure 5

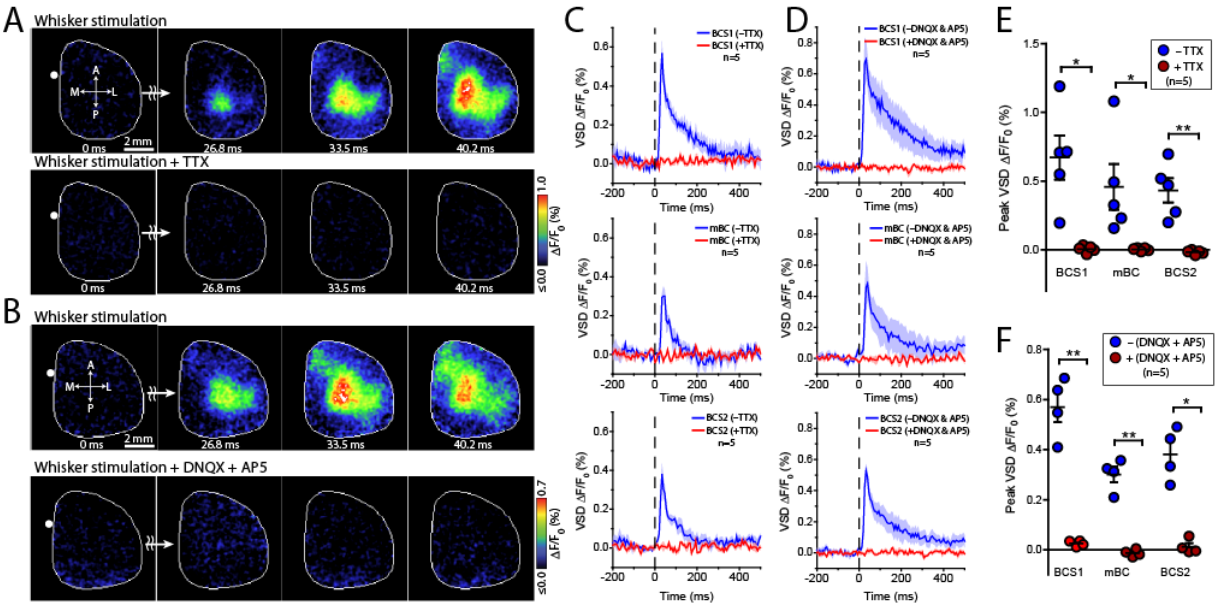

Supplementary Figure 5. Pharmacological blockade of sensory-evoked activity in the cortex.

(A) Montage of cortical VSD response following sensory stimulation of the contralateral whisker involving activation of primary somatosensory barrel cortex associated with the C2 whisker (BCS1), secondary somatosensory barrel cortex associated with the C2 whisker (BCS2), and motor associated barrel cortex (mBC) prior to (top) and following (bottom) topical application of TTX (10 μM) and sampled at 6.7 ms intervals. Responses are the means of 10 trials of stimulation. Both montages are scaled to the indicated colour bar. (B) As in (A), but illustrating activity prior to (top) and following (bottom) treatment with DNQX (200 μM) and AP5 (500 μM). (C) Time-course of whisker stimulation-evoked VSD activity from 0.112 mm^2 ROIs measuring activity from BCS1 (top), mBC (middle), and BCS2 (bottom) prior to (blue lines)

and following (red lines) TTX treatment (n=5). Shaded areas represent S.E.M. (D), As in (C) but with treatment with DNQX and AP5 (n=5). (E) Summary of the blockade of whisker-evoked cortical VSD activity (*, $P<0.05$, paired t-test) from BCS1, mBC, and BCS2.

Supplementary Figure 6

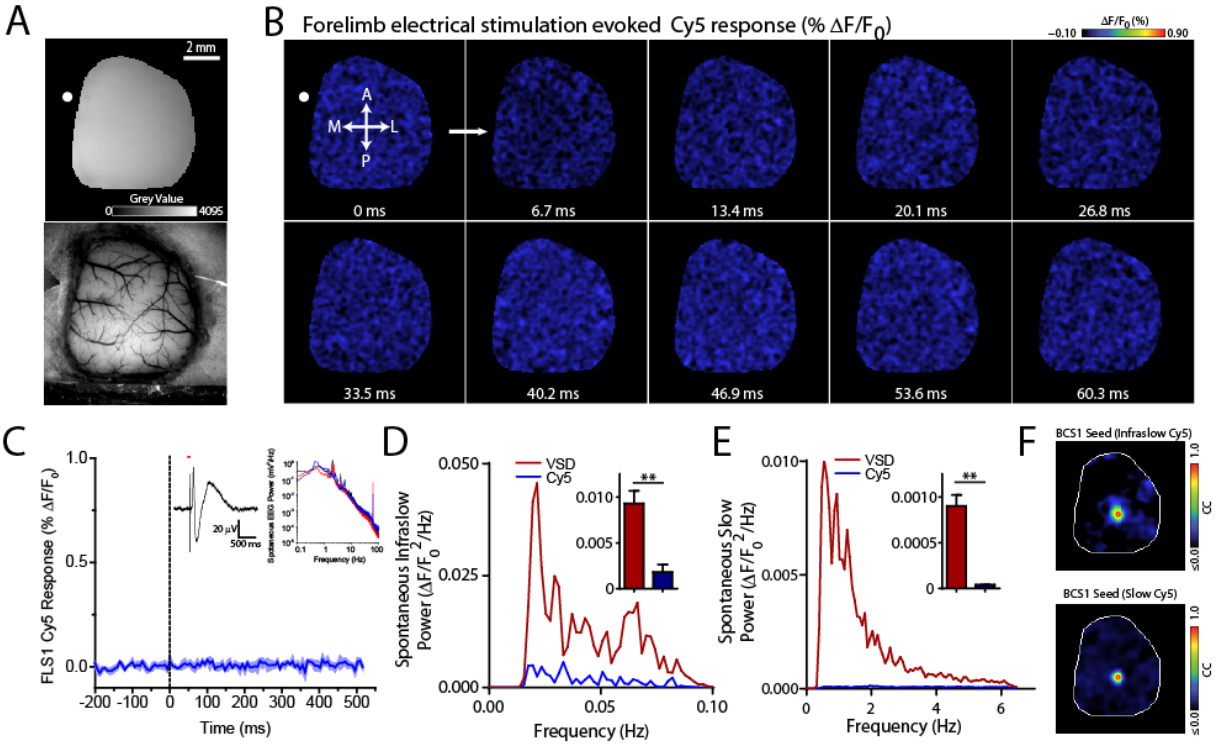

Supplementary Figure 6. Non-activity dependent Cy5 red fluorescence indicates minimal hemodynamic contribution to VSD signal

To rule out hemodynamic contribution to VSD signal, we used sulfo-Cyanine5 (Cy5; Lumiprobe), which exhibits similar spectral properties to RH-1692, is of similar molecular weight to RH1692 (RH1692=589, Cy5=665), is non-toxic, highly-water soluble, and exhibits no apparent voltage or otherwise intrinsic activity-dependence to its fluorescence. Cy5 (Lumiprobe) was dissolved in HEPES-buffered saline solution (0.5-1.0 mg/ml) and applied to the exposed cortex for 30-90 minutes. Cy5 fluorescence imaging began 30 minutes following washing of unbound Cy5.

Imaging acquisition and processing parameters were identical to VSD imaging. (A) Top, raw fluorescence of Cy5-dye-loaded cortex. Bottom, image of large, unilateral cranial window preparation depicted in A (Top). (B) Montage of sensory-evoked Cy5-fluorescence cortical response to strong electrical stimulation (1 ms, 1 mA) of contralateral forelimb. Electrical stimulus delivered at time 0 ms. (C) Group data from B illustrating negligible Cy5 fluorescence signal change ($\Delta F/F_0$) in response to electrical stimulation of the forelimb (N=3). Vertical dashed line indicates stimulus induction. Shaded blue area is S.E.M. Inset left, example of forelimb stimulation-evoked response detected by simultaneously recorded cortical surface EEG. Response is the mean of 10 trials. Red bar indicates stimulus delivery. Inset right, power spectrum indicating normal spontaneous EEG power recorded from mice whose cortices were labeled with Cy5 dye (n=3, each line represents an individual mouse). (D) Power spectra of infraslow (0.02-0.08 Hz) spontaneous VSD (red) and Cy5 (blue) fluorescence change ($\Delta F/F_0$) recorded from 25-30 minutes of activity from an ROI (0.112 mm^2) centered on BCS1. Inset, mean integrated power of spontaneous infraslow fluorescence change (n=3 mice, **, $P<0.01$, Student's t-test). (E) As in D, but for slow (0.5-6.0 Hz) spontaneous VSD and Cy5 fluorescence change ($\Delta F/F_0$). Inset, mean integrated power of spontaneous slow fluorescence change (N=3 mice, **, $P<0.01$, Student's t-test). (F) BCS1 seed correlation map generated from infraslow spontaneous Cy5 fluorescence (top) and slow spontaneous Cy5 fluorescence (bottom) indicating the presence of high correlation only surrounding the seed pixel. For display image in F, principal component analysis (PCA) was used to remove craniotomy window edge artifact.

Supplementary Figure 7

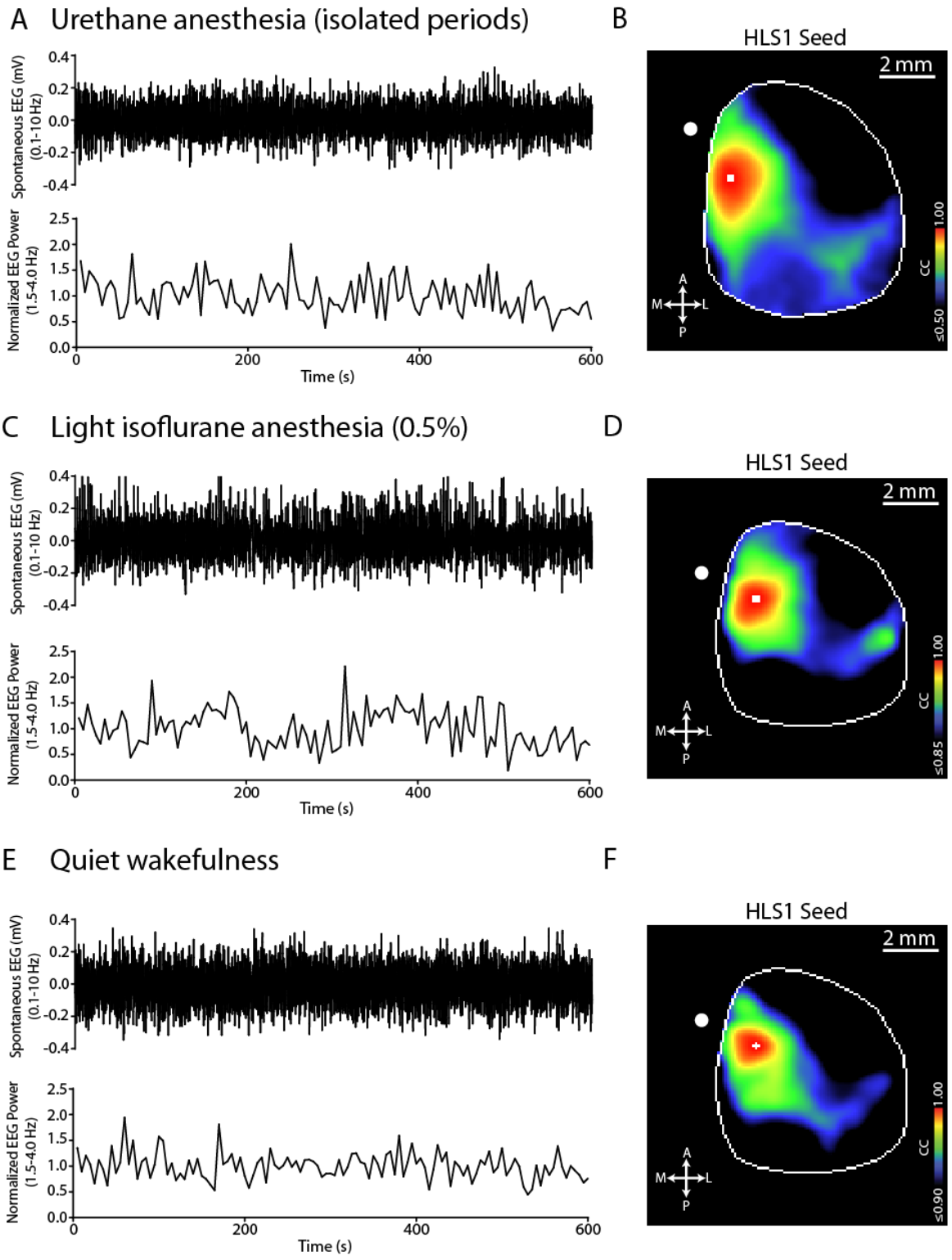

Supplementary Figure 7. Persistent infraslow (0.02-0.08 Hz) functional organization across brain states in the absence of cyclic ultraslow transitions

(A) Top, EEG (0.1-10 Hz) recording of spontaneous activity from a urethane-anesthetized mouse where spontaneous cyclic ultraslow transitions have been isolated and removed. Bottom, Delta (1.5-4.0 Hz) power of the EEG recording in (A, Top) illustrating the absence of cyclic ultraslow transition. (B) Infraslow functional connectivity demonstrated by a seed-map (HLS1) illustrating local and remote connections using only the spontaneous activity shown in A. (C) and (D), as in (A) and (B), but obtained from a lightly anesthetized mouse using isoflurane (0.5%) wherein spontaneous cyclic ultraslow transitions are absent. (E) and (F), as in (A) and (B), but from a mouse in a state of quiet wakefulness whereby spontaneous cyclic transitions are absent.